1   **Productivity and evapotranspiration of two contrasting semiarid ecosystems**
2   **following the 2011 global carbon land sink anomaly**

3   James CLEVERLY*[a,b], Derek EAMUS[a,b], Eva VAN GORSEL[c], Chao CHEN[a,1], Rizwana
4   RUMMAN[a], Qunying LUO[d], Natalia RESTREPO COUPE[d], Longhui LI[a], Natascha
5   KLJUN[e], Ralph FAUX[a], Qiang YU[a] and Alfredo HUETE[d]

6   [a] School of Life Sciences, University of Technology Sydney, PO Box 123, Broadway,
7   NSW, 2007, Australia

8   [b] Australian Supersite Network, Terrestrial Ecosystem Research Network, University of
9   Technology Sydney, PO Box 123, Broadway, NSW, 2007, Australia

10   [c] CSIRO Oceans and Atmosphere, Forestry House, Building 002, Wilf Crane Crescent,
11   Yarralumla, ACT 2601, Australia

12   [d] Climate Change Cluster, University of Technology Sydney, PO Box 123, Broadway,
13   NSW, 2007, Australia

14   [e] Department of Geography, Swansea University, Singleton Park, Swansea SA2 8PP, UK

15   *Correspondence: James.Cleverly@UTS.edu.au, +61 (02) 9514 8405, +61 (02) 9514
16   4079 (FAX)

17   **Keywords:** *Corymbia* **savanna;** *Acacia* **woodland; evapotranspiration; net**
18   **ecosystem productivity; water-use efficiency; global 2011 land**
19   **sink anomaly**
20

[1] Present address: CSIRO Agriculture Flagship, PMB 5, PO Wembley, WA, 6913, Australia

21 **ABSTRACT**

22   Global carbon balances are increasingly affected by large fluctuations in

23 productivity occurring throughout semiarid regions. Recent analyses found a large C

24 uptake anomaly in 2011 in arid and semiarid regions of the southern hemisphere.

25 Consequently, we compared C and water fluxes of two distinct woody ecosystems (a

26 Mulga (*Acacia*) woodland and a *Corymbia* savanna) between August 2012 and August

27 2014 in semiarid central Australia, demonstrating that the 2011 anomaly was short-lived

28 in both ecosystems. The Mulga woodland was approximately C neutral but with periods

29 of significant uptake within both years. The extreme drought tolerance of *Acacia* is

30 presumed to have contributed to this. By contrast, the *Corymbia* savanna was a very large

31 net C source (130 and 200 g C m^{-2} yr^{-1} in average and below average rainfall years,

32 respectively), which is likely to have been a consequence of the degradation of standing,

33 senescent biomass that was a legacy of high productivity during the 2011 anomaly. The

34 magnitude and temporal patterns in ecosystem water-use efficiencies (WUE), derived

35 from eddy covariance data, differed across the two sites, which may reflect differences in

36 the relative contributions of respiration to net C fluxes across the two ecosystems. In

37 contrast, differences in leaf-scale measures of WUE, derived from ^{13}C stable isotope

38 analyses, were apparent at small spatial scales and may reflect the different rooting

39 strategies of *Corymbia* and *Acacia* trees within the *Corymbia* savanna. Restrictions on

40 root growth and infiltration by a siliceous hardpan located below *Acacia*, whether in the

41 Mulga woodland or in small Mulga patches of the *Corymbia* savanna, impedes drainage of

42 water to depth, thereby producing a reservoir for soil moisture storage under *Acacia* while

43 acting as a barrier to access of groundwater by *Corymbia* trees in Mulga patches, but not

44 in the open *Corymbia* savanna.

45

1. Introduction

Inter-annual variability in atmospheric concentrations of CO_2 is large (Le Quéré et al., 2014), and much of this variability is driven by fluctuations in the source/sink strength of terrestrial ecosystems (Cox et al., 2013). During the latter half of the twentieth century, global net primary productivity (NPP) may have increased (Nemani et al., 2003), resulting in a potential increase in uptake of 0.05 Pg C per year (Ballantyne et al., 2012). Then, global NPP was reduced by 0.55 Pg C during the period 2000–2009, a result ascribed to large-scale drought in the southern hemisphere (Zhao and Running, 2010). Thereafter, Le Quéré et al. (2014) identified the 2011 land sink anomaly, which was a year of exceptional productivity, and Poulter et al. (2014) confirmed this anomaly by using a combination of modelling and remote sensing approaches. This land sink anomaly was driven by growth in semiarid vegetation of the southern hemisphere, with almost 60% occurring in Australia (Poulter et al., 2014). Importantly, Fasullo et al. (2013) showed that Australia, unlike continental South and North America, maintained a positive water mass anomaly (i.e., the extra water received in 2011 remained detectable throughout 2012), suggesting that increased C uptake may have persisted beyond 2011 in arid Australia. Carry-over of water from one hydrologic year to the next has been shown to have strong positive effects on productivity in many arid ecosystems (Flanagan and Adkinson, 2011). We have previously shown, using field observations of landscape fluxes of CO_2, that one of the dominant ecosystems of semiarid central Australia was indeed a large sink for C over almost all of the 12 months between October 2010 and October 2011 (Cleverly et al., 2013a; Eamus et al., 2013). Large fluctuations in productivity, evapotranspiration (ET) and ecosystem water-use efficiency (eWUE) across these semiarid regions reflect the very high ecosystem resilience of vegetation (Ponce Campos et al., 2013), which can have large

70 effects on global C relations and consequently drive events such as the land sink anomaly

71 of 2011.

72   Globally, dryland regions (arid, semiarid, and subhumid) cover 41% of the land

73 area (Reynolds et al., 2007). Within these regions, arid and semiarid environments are

74 characterised by chronic water shortages. Thus, productivity and ET are closely

75 dependent upon the timing, frequency and amount of precipitation (Huxman et al., 2004),

76 through which plant water availability is mediated by local hydrology (Breshears et al.,

77 2009; Loik et al., 2004; Reynolds et al., 2004).

78   The semiarid regions of Australia cover 70% of the continent (Eamus et al., 2006;

79 Warner, 2004) and are dominated by three major biomes along a woodland-savanna-

80 grassland continuum: (1) Mulga woodlands (*Acacia* spp.), which cover approximately

81 20–25% of the continental land area (Bowman et al., 2008), and (2) *Corymbia* savanna

82 over a hummock grass (*Triodia* spp.) understorey that grades into (3) treeless hummock

83 grasslands. Hummock grasslands and savannas occupy another 20–25% of the Australian

84 land surface (Bowman et al., 2008). The co-occurrence of two widely distributed and

85 highly distinctive vegetation types (i.e., Mulga and hummock) within a single climate

86 zone in central Australia (O'Grady et al., 2009) provides an opportunity to compare and

87 contrast their behaviour and to establish their respective contributions to regional C, water

88 and energy budgets.

89   Mulga trees range in height (2–10 m) and ground cover (10–70%) (Nix and

90 Austin, 1973), and they are preferentially located where storage of soil moisture occurs

91 near the surface in sand dunes, clay-rich soil or over the siliceous hardpans that are

92 common across semiarid Australia (Bowman et al., 2007; Ludwig et al., 2005; Maslin and

93 Reid, 2012; Nano and Clarke, 2010; Nix and Austin, 1973; Thiry et al., 2006; Tongway

94 and Ludwig, 1990). In contrast, tree density (stems per hectare) and cover in *Corymbia*

95   savannas are very low, and tree height ranges from 5–15 m. *Corymbia opaca* is deep-

96   rooted (8–20 m), and tends to be groundwater dependent in semiarid areas (Cook and

97   O'Grady, 2006; O'Grady et al., 2006a; O'Grady et al., 2006b). The understory in the

98   *Corymbia* savanna is characterised by a continuous cover of perennial hummock grasses

99   (*Triodia* spp.), which are widespread throughout Australia and cover an additional 20–

100 25% of the continental land area (Bowman et al., 2008; Nano and Clarke, 2010; Reid et

101 al., 2008).

102   Water-use-efficiency (WUE) has traditionally been measured at leaf-scales (as the

103 ratio of net assimilation to transpiration), but eddy covariance measurements also allow

104 determination of ecosystem-scale WUE as the ratio of net ecosystem productivity (NEP)

105 to ET (eWUE; Eamus et al., 2013). Given the very large difference in LAI of the C_4 grass

106 understory between Mulga and *Corymbia* savannas, we hypothesised that ecosystem-scale

107 WUE of the two biomes would differ. Furthermore, given the large differences in

108 phyllode structure of the C_3 trees, comparisons of leaf-scale measures of WUE across two

109 co-occurring species within a *single* biome (i) provide information about C and water

110 economies and (ii) contribute to our understanding of hydraulic niche separation of co-

111 occurring species (Peñuelas et al., 2011) that cannot be addressed through eWUE.

112   The aim of this study was to investigate fluctuations in the fluxes of C and water

113 from iconic Australian semiarid vegetation in response to reductions in precipitation

114 subsequent to the 2011 land sink anomaly. In this manuscript we compare and contrast

115 the behaviour of two disparate arid-zone tropical ecosystems (Mulga woodland and

116 *Corymbia* savanna) in central Australia to address four over-arching questions: (a) did the

117 2011 anomaly persist into 2012/2013/2014 in either biome; (b) do these two contrasting

118 ecosystems respond similarly to almost identical weather patterns; (c) how do ecosystem

119 water-use efficiencies compare across ecosystems; and (d) at small spatial scales within

120   the *Corymbia* savanna, how do leaf-scale water-use efficiencies across the two tree species

121   (*Acacia* and *Corymbia*) differ?

122

123   **2. Materials and Methods**

124   **2.1. Site descriptions**

125   This study was located on Pine Hill cattle station in the Ti Tree catchment of

126   central Australia and was co-located with several previous hydrological, ecological and

127   ecophysiological studies (Calf et al., 1991; Cleverly et al., 2013a; Eamus et al., 2013;

128   Harrington et al., 2002; Ma et al., 2013; O'Grady et al., 2009; Scanlon et al., 2006). The

129   Ti Tree catchment is an enclosed basin that covers 5,500 km^2 and contains two main

130   ecosystems: Mulga woodlands and *Corymbia* savanna (Harrington et al., 2002).

131   Measurements were collected from two locations: one in the Mulga woodland and one in

132   the *Corymbia* savanna. An eddy covariance tower was located in each ecosystem,

133   separated by 40 km at the same latitude ([22.3 °S 133.25 °E] and [22.3 °S 133.65 °E]).

134   A full description of the soil, floristics, leaf area index (LAI), energy balance and

135   C relations of the Mulga woodland can be found in Cleverly et al. (2013a) and Eamus et

136   al. (2013). Briefly, the Mulga woodland is characterised by a discontinuous canopy of

137   short (3–7 m), evergreen *Acacia* trees (*A. aptaneura* and *A. aneura*) with an understorey

138   of shrubs, herbs and grasses (C$_3$ and C$_4$) that are conditionally active depending upon

139   moisture availability and season (Cleverly et al., 2013a). The cover of *Acacia* is 74.5 % of

140   the land area in the Mulga woodland; *C. opaca* is essentially absent from the Mulga

141   woodland (one tree within the EC footprint, cf. Section 2.2). The basal area of *Acacia*

142   within the woodland is 8 m^2 ha^{-1} (Eamus et al., 2013).

143   The second eddy covariance site contains two species of trees: widely spaced and

144   tall *Corymbia opaca* trees above a matrix of hummock grass (Spinifex, *Triodia schinzii*)

145 and small patches of Mulga (*A. sericophylla*, *A. melleodora* and *A. aptaneura*) that contain

146 an understorey of herbs and tussock grasses (*Aristida* spp., *Eremophila latrobei* subsp.

147 *glabra*, *Eragrostis eriopoda* subsp. *red earth*, *Paraneurachne muelleri* and *Psydrax*

148 *latifolia*). Although the distribution of *T. schinzii* does not substantially overlap with

149 Mulga, *C. opaca* trees were present in both habitats. Representing only 0.4 % cover

150 (basal area of 0.21 m^2 ha^{-1}), *C. opaca* are found predominantly in the open savanna,

151 although they are found occasionally in the isolated small Mulga patch close to the EC

152 tower within in the *Corymbia* savanna. Soil texture is sandier in the *Corymbia* savanna

153 (loamy sand) than in the Mulga woodland (sandy loam). Soil organic matter is less than

154 1% at both sites. In the *Corymbia* savanna, the energy balance ratio $(H + LE)/(R_n - G)$

155 was 0.97 ± 0.005 (January 2013–July 2014), wherein H is sensible heat flux, LE is latent

156 heat flux, R_n is net radiation and G is ground heat flux. Over the same period in the Mulga

157 woodland, the energy balance ratio was 0.89 ± 0.005. The Bowen ratio (H/LE) was large

158 at both sites: 37.5 (range 0.78–408) in the Mulga woodland and 37.9 (0.23–511) in the

159 *Corymbia* savanna.

160 Long-term annual average precipitation (1987–2014) at the nearest meteorological

161 station (Territory Grape Farm, 18 km due south of the *Corymbia* savanna site) is 320.7

162 mm (http://www.bom.gov.au). The monsoon tropics of Australia are defined by the

163 receipt of 85% of annual precipitation during the November–April monsoon season

164 (Bowman et al., 2010), which places these sites within the monsoon zone on average

165 (Cleverly et al., 2013a). However, during the first 16 months of this study (August 2012–

166 November 2013), very little rain was received and there was consequently negligible

167 grassy understorey, in contrast to the extensive understorey that was present during the

168 land sink anomaly of 2011 (Eamus et al., 2013).

169

2.2. Eddy covariance data

Eddy covariance analyses of NEP and ET were used as measures of net C uptake and ecosystem water use. In the eddy covariance method, ET is determined from the covariance between vertical wind speed (w) and specific humidity (q): $ET = <w'q'>/\rho_w$, where $<>$ represents an average in time and the prime operator represents the deviation from a mean: $q' = <q> - q_i$. Similarly, NEP was taken to be the negative covariance between w and [CO_2] (c): $NEP = -<w'c'>$. By this definition, NEP is positive during C uptake (i.e., photosynthesis, C sink) and negative for net C emissions (C source). The trade-off between C uptake and ET was represented by eWUE, which was calculated as the ratio of NEP and ET. Because of non-linearity at very small values of ET, eWUE was determined only when ET was larger than 0.2 mm d^{-1}.

Both tower sites are part of the OzFlux Network (Cleverly, 2011; Cleverly, 2013). The 90% flux footprint (Kljun et al., 2004) under turbulent conditions extended 200–300 m to the southeast of either tower, although variability in roughness length across the *Corymbia* savanna interferes with the reliability of footprint estimates at that site. In the *Corymbia* savanna, approximately 25% of the flux footprint covered the *Corymbia* savanna, while the remaining 75% of the footprint was located over the small Mulga patch that included *Acacia*, *Corymbia* and tussock grasses. The trees nearest the tower in the open *Corymbia* savanna are *Acacia* with a canopy height of 4.85 m, in contrast to the 6.5 m tall *Acacia* in the Mulga woodland. Thus, measurements were made over the *Corymbia* savanna at a slightly lower height (9.85 m) than above the Mulga woodland (11.6 m, Cleverly et al., 2013a). Where possible, the instruments on each tower were the same (e.g., Campbell Scientific CSAT3) or only different in the model of sensor (e.g., Kipp & Zonen CNR1 *v.* CNR4, Li-Cor 7500 *v.* 7500A), in which the newer models were used in the *Corymbia* savanna.

195   All estimates of error were determined as the standard error (s.e. $= \sigma / n^{0.5}$, where σ

196   is the standard deviation and n is sample size).

197

198   **2.2.1. Quality control, corrections and gap-filling**

199   Quality control of meteorological and flux measurements (QA/QC) was performed

200   on both towers as described in Eamus et al. (2013). Briefly, QA/QC procedures included

201   spike detection and removal, range checks that include rejection of measurements when

202   the wind was from a 90° arc behind the sonic anemometer (CSAT3) and tower (10% of

203   observations, only during the passage of frontal systems that generate advection and

204   negative fluxes of LE; Beringer and Tapper, 2000), and filtering for bad measurements of

205   humidity from the IRGA in comparison to a slow-response sensor. Corrections included

206   2-dimensional coordinate rotation (Wesely, 1970), frequency attenuation correction for

207   time averaging and sensor displacement (Massman and Clement, 2004), conversion of

208   virtual to actual sensible heat flux (Campbell Scientific Inc., 2004; Schotanus et al., 1983),

209   correction for flux-density effects (the Webb, Pearman and Leuning correction, which

210   accounts for density effects arising from heat and water vapour fluxes; Webb et al., 1980)

211   and storage of heat in the soil above the ground heat flux plates. Corrections and QA/QC

212   steps were performed using OzFluxQC and the OzFluxQC Simulator, both in version

213   2.8.5 and available online (e.g., Cleverly and Isaac, 2015). Gaps in fluxes were filled

214   using a self-organising linear output (SOLO) that was trained on a self-organising feature

215   map (SOFM) of meteorological (net radiation, air temperature, vapour pressure deficit,

216   specific humidity) and soil measurements (G, soil temperature, soil moisture content at the

217   surface) (Eamus et al., 2013). SOLO is a statistical artificial neural network (ANN) and

218   was chosen for its resistance to overtraining (Hsu et al., 2002), ability to simulate fluxes

219 (Abramowitz et al., 2006), and small RMSE relative to feed forward ANNs (Eamus et al.,

220 2013).

221   In contrast to gaps in the flux measurements, two types of gaps were identified in

222 the meteorological data: those that were due to measurement over-ranging on the

223 datalogger and those that occurred during system maintenance. Over-ranging was

224 identified in the measurement of solar radiation during periods when reflection from a

225 cloud face generated large (> 1200 W m^{-2}) radiant fluxes. To avoid underestimation bias

226 in these cases, gaps in 30-minute solar (R_s) and net (R_n) radiation were filled from the

227 measured value in each minute that did not report an over-ranging error (26–29 one-

228 minute values). These gaps first occurred during the summer 2012–2013 at the *Corymbia*

229 savanna site, after which modifications to the datalogger prevented re-occurrence of solar

230 spike gaps.

231   System maintenance gaps were typically 30–300 minutes and did not coincide

232 among sites. Filling of gaps in the meteorological variables that were used as predictors

233 for gap filling of fluxes was performed using several methods: 1) linear interpolation, 2)

234 replacement of measurements from the companion tower, and 3) SOLO-SOFM trained on

235 measurements from the paired tower. Gaps in meteorological measurements were filled

236 using the method that produced the smallest disjunction at gap boundaries.

237

238 **2.3. Trends in satellite derived enhanced vegetation index (EVI) for the two sites**

239   The moderate resolution imaging spectroradiometer (MODIS) enhanced vegetation

240 index (EVI) is sensitive to vegetation "greenness" (i.e., chlorophyll content) and structural

241 properties (e.g., LAI, canopy type, plant physiognomy, canopy architecture) (Huete et al.,

242 2002). Thus, the satellite product MODIS EVI was used in this study to assess structural

243 and functional responses of the vegetation. The MOD13Q1 product was retrieved from

244 the ORNL DAAC depository at a temporal resolution of 16 days and a spatial resolution

245 of 250 m. Values were composited into a single 9×9 pixel centred on each tower (2.25

246 km resolution, only pixels that passed QA at 100% were used). The MODIS satellite was

247 launched in 2000, and we present the entire record to provide context for the ecosystem

248 dynamics observed over this two-year study.

249

250 **2.4. ^{13}C foliar stable isotopes**

251 To compare leaf-scale intrinsic WUE (WUE$_i$) at small spatial scales within the

252 *Corymbia* savanna, leaf samples were collected in September 2013 for analysis of the

253 stable isotope ratio of C ($\delta^{13}C$). Mature leaves of *Corymbia opaca* and *Acacia* trees were

254 collected from three habitats within the *Corymbia* savanna. The first habitat was from the

255 *Corymbia* savanna *per se*; the second habitat was the small Mulga patch close to the EC

256 tower within the *Corymbia* savanna; the third habitat was the transition between the small

257 Mulga patch and the *Corymbia* savanna. For comparison with *Acacia* sampled within the

258 *Corymbia* savanna, $\delta^{13}C$ of bulk leaf tissue was also measured in the Mulga woodland

259 from two replicate branches of three replicate trees of *Acacia*.

260 In *Corymbia*, three leaves from different branches were collected. Each leaf was

261 ground and subsampled to obtain three representative independent values per tree.

262 Likewise, *Acacia* phyllodes were sampled from three different branches, although several

263 phyllodes were combined from each branch due to their small size. The C isotopic

264 composition was measured using a Picarro G2121-i Analyser for Isotopic CO_2 (Picarro

265 Inc., Santa Clara CA USA). Atropine and acetanilide were used as internal reference

266 standards and calibrated against international measurement standards sucrose (IAEA-CH-

267 6, $\delta^{13}C_{VPDB} = -10.45$ ‰), cellulose (IAEA-CH-3, $\delta^{13}C_{VPDB} = -24.72$ ‰) and graphite

268 (USGS24, $\delta^{13}C_{VPDB} = -16.05$ ‰). Values of $\delta^{13}C$ in bulk leaf samples represent an

269 integrated value of C_i/C_a (i.e., the ratio of internal leaf and atmospheric CO_2 density)

270 during the entire age of the leaf.

271

272 **3. Results**

273 **3.1. Water fluxes: daily, seasonal and annual precipitation**

274   Daily rainfall across the two-year period showed minimal differences between the

275 Mulga woodland and *Corymbia* savanna sites (Fig. 1a, b). Rainfall in both years was

276 concentrated between November and early May, although both sites received about 12

277 mm of rain in July 2014. During the first year of this study (2013–2014), rainfall during

278 the monsoon season (November–April) was 71 and 74% of total annual rainfall for that

279 year in the Mulga woodland and *Corymbia* savanna, respectively. In the following year,

280 rainfall during the monsoon season was 92% of total annual rainfall at both sites.

281 Although these sites are within the monsoon zone on average (Cleverly et al., 2013a), the

282 monsoon did not penetrate inland to the location of these sites in the first year of the

283 present study (August 2012–July 2013). Due to the proximity between sites, annual

284 rainfall did not differ in either of the two years of the present study. Likewise, due to

285 cross-correlation between precipitation *versus* temperature (maximum, mean, minimum),

286 solar radiation and vapour pressure deficit (Cleverly et al., 2013a), meteorological

287 conditions were equivalent across sites (data not shown).

288   In the 2010–2011 hydrological year (August–July), annual rainfall (565 mm) was

289 significantly larger than the long-term average of 320.7 mm (Table 1). In contrast, annual

290 rainfall was smaller than average in hydrological years 2011–2013 (Table 1). During the

291 first year of this study (August 2012–July 2013), annual rainfall was approximately 40%

292 less than the long-term average (192.8 and 190.6 mm in the Mulga woodland and

293 *Corymbia* savanna, respectively). In the second year of this study (2013–2014), rainfall

294 was 294.6 and 289.8 mm in the Mulga woodland and *Corymbia* savanna, respectively

295 (approximately 8% below the long-term average). Monthly patterns and cumulative

296 annual (August–July) rainfall in the first year of study were almost identical at the two

297 sites (Fig. 1c). In contrast there was more rain earlier in the second hydrologic year

298 (November 2013–February 2014) at the *Corymbia* savanna than the Mulga woodland,

299 although annual totals for the two sites did not differ.

300

301 **3.2. Water fluxes: evapotranspiration**

302   Patterns in daily ET were similar across the two-year study at both sites (Fig. 2a)

303 and closely followed those observed for rainfall. Daily ET at both sites was negligible

304 during those periods when daily rainfall was zero for more than two weeks (e.g., August

305 2012 and 2013, June 2014). Maximum rates of daily ET from the *Corymbia* savanna were

306 either equal to or frequently larger (by up to approximately 80%) than those from the

307 Mulga woodland (Fig. 2a). Summer total and maximum daily rates of ET were larger in

308 the second summer than in the first at both sites. As with rainfall, 73 and 88% of ET was

309 lost from the Mulga woodland during the first and second monsoon seasons, respectively.

310 Likewise in the *Corymbia* savanna, 71 and 91% of ET was lost during the respective

311 monsoon seasons.

312   In both hydrologic years (August 2012–July 2014), patterns of cumulative ET

313 were broadly similar at the two sites, but with a consistent difference in the total amount

314 of ET (Fig. 2b). Moreover, the annual sum of ET was smaller for the Mulga woodland

315 than the *Corymbia* savanna in both years. The annual total ET for the *Corymbia* savanna

316 was 96 and 110% of annual rainfall in each year (2012–2013 and 2013–2014,

317 respectively), but in the Mulga woodland the annual sum of ET was approximately 80%

318 of total rainfall in both years (cf. Figs. 1c and 2b). Immediately following precipitation,

319   there were larger pulses of ET from the *Corymbia* savanna than from the Mulga woodland

320   (cf. Figs. 1c and 2a). These short imbalances were more prominent in the second year,

321   when ET was 110% of precipitation in the *Corymbia* savanna.

322

323   **3.3. Carbon fluxes: net productivity and water-use efficiency**

324   In contrast to the very similar patterns in daily ET at both sites, patterns in daily

325   NEP differed substantially between the two sites (Fig. 3a). During the winter and early

326   spring (August–October) of 2012, the Mulga woodland was a small sink (NEP = 0.1 to 0.3

327   g C m^{-2} d^{-1}), but the *Corymbia* savanna was a moderate source for C (NEP = −0.6 to −0.3

328   g C m^{-2} d^{-1}). This pattern was repeated in the second winter/early spring (June–August

329   2013). The *Corymbia* savanna remained a moderate-to-strong source (NEP = −1.75 to

330   −0.5 g C m^{-2} d^{-1}) between November 2012 and January 2014, with the exception of a

331   short period during June 2013 when the *Corymbia* savanna became C neutral (uptake

332   equalled release) (Fig. 3a). The *Corymbia* savanna was a sink for C (maximum daily NEP

333   = 1.5 g C m^{-2} d^{-1}) for approximately six weeks in the summer of 2014 (late January to

334   early March). The Mulga was a moderate-to-large C source for the spring and early

335   summer of 2014 and became a moderate sink (maximum NEP = 0.75 g C m^{-2} d^{-1}) in late

336   summer and autumn of 2014 (Fig. 3a).

337   During summer in the *Corymbia* savanna, the pulse of productivity was rapid and

338   large following the largest storm in the two years of study (> 100 mm in January 2014; cf.

339   Figs. 1 and 3a), and this was due to the dominant cover of C_4 grasses (90%). By contrast

340   in the Mulga woodland, productivity was limited during the summer, acting as a source

341   for several weeks until late summer and early autumn of 2014 (Fig. 3a). In contrast, both

342   sites were a C source in January 2013 (Fig. 3a). During this time, ecosystem respiration at

343   night was similarly small in the Mulga woodland and *Corymbia* savanna (Fig. 4).

14

344 However, during the sunlit hours, NEP diverged between the two sites. By example in

345 January 2013 the Mulga woodland was a net C source. However, in the mornings of

346 January, a positive NEP (C sink, reflecting a stimulation of photosynthetic C uptake

347 through increased solar radiation input) was recorded, followed by a rapid decline from

348 mid-morning through to early evening (Fig. 4). NEP was negative (C source) prior to

349 sundown. By contrast, NEP was consistently negative in the *Corymbia* savanna, which

350 was a stronger C source during daylight hours than at night, reflecting the enhanced rates

351 of C emissions that occurred during sunlit hours in the savanna.

352   Cumulative annual NEP in both hydrologic years showed the *Corymbia* savanna to

353 be a strong source (cumulative NEP $= -197$ and -131 g C m^{-2} y^{-1} for the first and second

354 years, respectively; Fig. 3b). In contrast, the Mulga woodland was a small source (-26 g

355 C m^{-2} y^{-1}) in the first hydrologic year but a small sink (12 g C m^{-2} y^{-1}) in the second year.

356 It wasn't until the occurrence of a wet summer that the Mulga woodland again became a

357 moderate-to-strong sink (0.9 g C m^{-2} d^{-1}), although annual C uptake was considerably less

358 than that observed in the 2010–2011 anomaly (12 *versus* 259 g C m^{-2} y^{-1}), reflecting the

359 non-linear response of NEP to total annual rainfall in this system. The trend in cumulative

360 NEP at the two sites diverged in early March 2014, with the *Corymbia* savanna reverting

361 to a source for the remaining five months of the study and the Mulga continuing as a net

362 sink (Fig. 3b).

363   In the *Corymbia* savanna, eWUE was negative (negative because respiratory loss

364 exceeded photosynthetic C gain) for most of the two years of study (Fig. 5) and was more

365 negative in the first hydrologic year than the second. Periods of very small positive or

366 slightly negative eWUE for the *Corymbia* coincided with the rainfall of November 2012–

367 February 2013, May 2013 and January–March 2014. In contrast, the Mulga woodland

368 maintained near-zero values of eWUE in both years, although eWUE increased gradually

369 in autumn (March – May) as soil water stores that were recharged during the wet season

370 declined following the cessation of summer rainfall (Fig. 5).

371

372 **3.4. Trends in enhanced vegetation index and foliar ^{13}C stable isotope contents**

373 MODIS EVI exhibited strong peaks at the study sites in five of 13 years since the

374 launch of the satellite: March 2000, April 2001, April 2007, March 2010 and March 2011

375 (Fig. 6). In a given year, neither ecosystem consistently responded to precipitation with

376 more production of green tissue than the other (Fig. 6). While MODIS EVI was generally

377 larger in the Mulga woodland than in the *Corymbia* savanna, two periods (2004 and 2010)

378 when this pattern was reversed are apparent (Fig. 6). Note that during the first year of this

379 study (2012–2013), MODIS EVI values were the smallest on record for the Mulga

380 woodland and as small as previous minima in the *Corymbia* savanna (2008, 2009).

381 In *Acacia* phyllodes, $\delta^{13}C$ values averaged −27.9‰ and did not differ substantially

382 across the two sites and in the three habitats sampled within the *Corymbia* savanna. By

383 contrast, $\delta^{13}C$ in *Corymbia opaca* leaves declined substantially across habitats (Fig. 7).

384 Leaf $\delta^{13}C$ of the *Corymbia* trees declined in the sequence: *Corymbia* trees in the Mulga

385 patch within the *Corymbia* savanna > *Corymbia* trees in the transition between the *Acacia*

386 patch and open *Corymbia* savanna > *Corymbia* trees in the extensive open savanna (Fig.

387 7). Leaf $\delta^{13}C$ in *Corymbia* was less negative than in *Acacia* phyllode in the Mulga patch

388 (Fig. 7).

389

390 **4. Discussion**

391 **4.1. The 2011 anomaly and beyond**

392 Although measurements were not initiated in the *Corymbia* savanna until after the

393 conclusion of the land sink anomaly, C fluxes in subsequent years can only be explained

394   within the context of the land sink anomaly. Several lines of field-based evidence support

395   the conclusion (Le Quéré et al., 2014; Poulter et al., 2014) that Australian semi-arid

396   vegetation had a major role in the large global land sink anomaly of 2011. First, our field-

397   based studies of CO_2 fluxes in central Australia (Table 1; Eamus et al., 2013)

398   demonstrated that the Mulga woodland was indeed a large sink for C (259 g C m^{-2} y^{-1},

399   Table 1) during that year (September 2010–August 2011; Eamus et al., 2013). This sink

400   formed in response to a disproportionate increase in gross primary production (GPP, 793 g

401   C m^{-2} y^{-1}) relative to the moderate increase in ecosystem respiration (Cleverly et al.,

402   2013a). Second, the largest value of EVI since 2000 was observed in hydrologic year

403   2010–2011 (Ma et al., 2013), which suggests as large a C sink in the *Corymbia* savanna as

404   in the Mulga woodland due to the close correlation between EVI and GPP across tropical

405   and semi-arid Australia (Donohue et al., 2014; Ma et al., 2013; Ma et al., 2014). Third,

406   2010–2011 was identified as having the largest rates of ET in the Ti Tree basin since 1981

407   (Chen et al., 2014). Finally, the Gravity Recovery and Climate Experiment (GRACE)

408   satellite data recorded significant increases in the amount of water stored across the

409   Australian landmass in 2011 (Boening et al., 2012), coincident with the extremely large

410   La Niña conditions that dominated weather across Australia in that year.

411   During the global land sink anomaly of 2011, rainfall at our sites was almost

412   double the long-term average (565 mm *versus* 320.7 mm, 1987–2014), resulting in very

413   large rates of ecosystem productivity in the Mulga woodland (Eamus et al., 2013) and the

414   *Corymbia* savanna (Fig. 6). Across a range of biomes, different combinations of rainfall,

415   temperature, solar radiation and vapour pressure deficit are the principle determinants of

416   NEP and GPP (Baldocchi, 2008; Baldocchi and Ryu, 2011; Kanniah et al., 2010; van Dijk

417   et al., 2005; Zha et al., 2013). It is apparent that inter-annual differences in precipitation

418   are the principle causes of interannual differences in sink strength for the Mulga woodland

419   (Table 1), in strong agreement with multiple other arid and semiarid biomes (Barron-

420   Gafford et al., 2012; Chen et al., 2014; Flanagan and Adkinson, 2011; Huxman et al.,

421   2004; Ma et al., 2012) but in marked contrast to boreal forests, tropical montane forests,

422   temperate mesic deciduous forests and tropical mesic savannas, where temperature, solar

423   radiation and the length of the growing season are the principal factors limiting NEP

424   (Baldocchi, 2008; Dunn et al., 2007; Keenan et al., 2014; Luyssaert et al., 2007; Ma et al.,

425   2013; Whitley et al., 2011; Zha et al., 2013). We now discuss the question: did this

426   anomaly persist into 2012–2014 for our two study sites?

427   Despite the persistence of anomalously large moisture reserves in Australia

428   through 2012 (Fasullo et al., 2013), the productivity pulse of 2011 (Eamus et al., 2013) did

429   not persist in either ecosystem following the conclusion of the 2011 global land C sink

430   anomaly. Productivity declined in the Mulga woodland by July 2011, which was four

431   months following the end of the summer rains (Cleverly et al., 2013a; Eamus et al., 2013),

432   and the Mulga woodland was effectively C neutral (i.e., near zero within the limits of

433   measurement uncertainty) in the three following years (2012–2014). The ratio of GPP to

434   ecosystem respiration fell between 2011 and 2012, reflecting a two-fold decline in annual

435   GPP (Cleverly et al., 2013a) and a four-fold decline in the seasonal peak of daily GPP (Ma

436   et al., 2013). Similarly, there was little evidence of productivity in the *Corymbia* savanna

437   during the first nine months of the current study (August 2012–May 2013). In pyrophytic

438   landscapes such as the *Corymbia* savanna, large amounts of fuel can accumulate following

439   very wet periods (King et al., 2013; Schlesinger et al., 2013). However, large rates of C

440   loss from this biome during subsequent dry years imply a rapid loss of fuel load via

441   photodegradation. Thus, *Corymbia* savannas that do not burn in the first few years

442   following very wet conditions are less likely to burn thereafter.

443

444 **4.2. *Corymbia* savanna *versus* Mulga woodland**

445 In this section, we address the question: how do current behaviours of the Mulga

446 woodland (in terms of CO_2 and water fluxes) compare to those of an adjacent, floristically

447 different, *Corymbia* savanna?

448   Some of the ET excess in the *Corymbia* savanna in the second year of study (ET =

449 110% of precipitation) arose from precipitation that fell during the first year but

450 contributed to second-year ET, while the remainder may illustrate the opportunistic use of

451 groundwater by *Corymbia* trees in the open savanna during short periods of cloud cover,

452 cool temperatures, and low VPD that accompany rainfall. What was perhaps surprising

453 was the continued ET deficit in the Mulga woodland (about 80% of annual rainfall) in the

454 very wet (2011) year (Eamus et al., 2013) and the subsequent dry years, with little

455 apparent use of water that was carried-over in soil storage, in marked contrast to the

456 generally positive effect of carry-over of water from one year to the next in arid zones

457 (Flanagan and Adkinson, 2011). However, the abundant sunshine and soil moisture

458 availability during the summer of 2013–2014 may suggest that ET was limited by

459 stomatal responses to high temperature and large VPD (Cleverly et al., 2013b) rather than

460 energy or water availability. Thus, recharge and discharge of soil moisture storage (and

461 the ratio of ET to precipitation) vary on longer timescales than the scope of our

462 measurements, in contrast to the intra-annual carry-over of water from the wet season into

463 the cool season observed in North American drylands (Hastings et al., 2005). In both

464 ecosystems, the increase in evaporative fraction (defined as the ratio of ET to net

465 radiation) from the first to the second summer was the result of higher ET and lower net

466 radiation during the second summer. This difference between summer seasons was the

467 consequence of disparities in the amount and temporal distribution of rainfall. In the

468   second summer, larger storms and fewer sunny days caused VPD to be much smaller, with

469   a consequential reduction in leaf stress.

470   The resilience of both ecosystems (*sensu* Ponce Campos et al., 2013, where

471   resilience is defined as ecophysiological drought tolerance that does not diminsh

472   photosynthetic responses to subsequent periods of favourable moisture availability)

473   resulted in large fluctuations of eWUE and a near-neutral annual C balance in the Mulga

474   woodland (Fig. 3 and Cleverly et al., 2013a), whereas the C cycle in the *Corymbia*

475   savanna was dominated by large C losses (Fig. 3). Two reasons may be postulated to

476   explain the difference in C balance of the two sites. First, *Acacia* has a suite of traits that

477   are indicative of a high degree of drought tolerance compared to *Corymbia*: larger wood

478   density, smaller specific leaf area (SLA, ratio of leaf area to leaf dry mass) and larger

479   Huber value (ratio of sapwood cross-sectional area to leaf area) (O'Grady et al., 2009).

480   Large wood densities are strongly correlated with enhanced resistance to xylem embolism,

481   reduced soil-to-leaf hydraulic conductance and small transpiration rates (Wright et al.,

482   2006; Zhang et al., 2009), while a small SLA correlates with an ability to tolerate lower

483   (more negative) canopy water potentials. As a result, small rates of productivity in the

484   Mulga woodland were sufficient for maintaining C neutrality. Second, woody plants

485   dominate the Mulga woodland, whereas the contribution of *Acacia* and *Corymbia* to the

486   cover, basal area and LAI of the *Corymbia* savanna is small relative to the extensive C_4

487   grasses. We propose that the large amount of standing dead biomass in the *Corymbia*

488   savanna (accumulated during the 2011 anomaly) was subject to physical fragmentation by

489   photodegradation (i.e., in the presence of light, e.g. Fig. 4, and absence of soil moisture;

490   Rutledge et al., 2010; Vanderbilt et al., 2008).

491

4.3. Ecosystem-scale water use efficiency (eWUE) and small-scale differences in foliar WUE (WUE$_i$)

By delaying production until the autumn of 2014, eWUE in the Mulga woodland was larger than in the *Corymbia* savanna. In addition to the traits of drought tolerance, which are correlated to large WUE, the large foliar N content of the nitrogen fixing *Acacia* allows for significant resource substitution, whereby larger-than-expected rates of photosynthesis can be sustained in arid environments through preferential allocations of nitrogen to Rubisco (Taylor and Eamus, 2008). When stomatal conductance and transpiration rates decline in response to large VPD, resource substitution results in large eWUE. Further, spatial variability in soil properties (especially the distribution of the hardpan) restricts soil moisture availability (Chen et al., 2014) and contributes to large values of eWUE in the Mulga woodland.

It is important to note that the eWUE of the Mulga woodland consistently showed that photosynthetic C uptake exceeded respiratory loss per unit ET during the early or late summer and autumn of both years, as previously observed by Eamus et al. (2013). The very low values of eWUE in the *Corymbia* savanna imply that C source strength was maintained regardless of moisture status, thus eWUE became much more negative during dry periods than eWUE in the Mulga woodland (Fig. 5). These predominantly large, negative values of eWUE (respiration exceeds C gain per unit ET) in the *Corymbia* savanna are further symptomatic of photodegradation. Despite the differences in eWUE between ecosystems and the plants that co-exist in them, eWUE in the Mulga woodland and the *Corymbia* savanna showed large fluctuations between wet and dry periods that reflected differences in the moisture requirements of photosynthesis, autotrophic and microbial respiration, and photodegradation.

516   In leaves of *Corymbia* across all three habitats, declining leaf $\delta^{13}C$ represents

517   increased access to water and declining WUE_i (Leffler and Evans, 1999; Zolfaghar et al.,

518   2014) and has been previously used to infer access to groundwater (Zolfaghar et al.,

519   2014). We interpret this as reflecting an increasing rooting depth of *Corymbia* trees

520   within the *Corymbia* savanna when moving into the extensive open savanna from the

521   Mulga patch. The potential for groundwater access by deeply rooted *Corymbia* in the

522   extensive savanna, where groundwater depth is approximately 8 m, is presumably large

523   and may explain the lower WUE_i of *Corymbia*, while the presence of an inferred hardpan

524   within the Mulga patch prevents access to the water table and hence an increased WUE_i

525   for *Corymbia* within the Mulga patch. The absence of any significant change in phyllode

526    $\delta^{13}C$ for the *Acacia* at any of the three locations within the *Corymbia* savanna reflects the

527   shallow rooting habit of *Acacia* (Pressland, 1975). More importantly, there was no

528   difference in foliar ^{13}C content of *Acacia* sampled from the Mulga woodland where

529   groundwater depth is known to exceed 50 m, further supporting the conclusion that access

530   to groundwater by Mulga within the *Corymbia* savanna is not occurring. The low values

531   of $\delta^{13}C$ in *Acacia* phyllodes are consistent with their anisohydric stomatal responses to soil

532   drying; that is, their stomata remain open even at very low water potentials (O'Grady et

533   al., 2009; Winkworth, 1973).

534

535   **5. Conclusions**

536   We have demonstrated that the large 2011 anomaly in terrestrial C uptake was

537   short-lived in the arid zone of central Australia. In the Mulga woodland, storage of soil

538   moisture within the root zone contributed to C neutrality (i.e., C sources were equivalent

539   to sinks) in the subsequent drier-than-average years by facilitating the delayed response of

540   productivity to precipitation. We also demonstrated that productivity in the Mulga

541   woodland was larger than that of the *Corymbia* savanna in the drier-than-average years of

542   the study and attributed this to the multiple drought tolerant attributes and the larger

543   potential for resource substitution of *Acacia* compared to *Corymbia*. Drought tolerance in

544   the Mulga woodland further restricted ET to 80% of precipitation in each year since 2010,

545   indicating that variations in soil moisture storage occur over very long timescales. In

546   contrast, ET from the *Corymbia* savanna was larger than precipitation in the near-average

547   rainfall year, illustrating that groundwater use by *Corymbia* occurred opportunistically

548   during wet periods. However, the *Corymbia* savanna was a strong source of CO_2 in drier-

549   than-average and near-average years due to photodegradation of the extensive grassy

550   understorey. Finally, we demonstrated that ecosystem water-use efficiency was larger in

551   the Mulga woodland than in the *Corymbia* savanna, while differences in leaf/phyllode

552     $\delta^{13}C$ between *Acacia* and *Corymbia* reflected differential access to groundwater and the

553   different rooting characteristics of these two tree species.

554

555

6. Acknowledgements

561

562

563

7. References

Abramowitz, G., Gupta, H., Pitman, A., Wang, Y., Leuning, R., Cleugh, H. and Hsu, K.L., 2006. Neural Error Regression Diagnosis (NERD): A tool for model bias identification and prognostic data assimilation. J. Hydrometeor. 7: 160–177.

Baldocchi, D., 2008. Breathing of the terrestrial biosphere: lessons learned from a global network of carbon dioxide flux measurement systems. Aust. J. Bot. 56: 1–26, DOI: 10.1071/BT07151.

Baldocchi, D.D. and Ryu, Y., 2011. A synthesis of forest evaporation fluxes – from days to years – as measured with eddy covariance. In: D.F. Levia, D. Carlyle-Moses and T. Tanaka (Editors), Forest Hydrology and Biogeochemistry: Synthesis of Past Research and Future Directions. Ecological Studies. Springer, Dordrecht, Netherlands, pp. 101–116, DOI: 10.1007/978-94-007-1363-5_5.

Ballantyne, A.P., Alden, C.B., Miller, J.B., Tans, P.P. and White, J.W.C., 2012. Increase in observed net carbon dioxide uptake by land and oceans during the past 50 years. Nature. 488: 70–73, DOI: 10.1038/nature11299.

Barron-Gafford, G.A., Scott, R.L., Jenerette, G.D., Hamerlynck, E.P. and Huxman, T.E., 2012. Temperature and precipitation controls over leaf- and ecosystem-level CO_2 flux along a woody plant encroachment gradient. Glob. Change Biol. 18: 1389–1400, DOI: 10.1111/j.1365-2486.2011.02599.x.

Beringer, J. and Tapper, N.J., 2000. The influence of subtropical cold fronts on the surface energy balance of a semi-arid site. J. Arid. Environ. 44: 437-450.

Boening, C., Willis, J.K., Landerer, F.W., Nerem, R.S. and Fasullo, J., 2012. The 2011 La Niña: So strong, the oceans fell. Geophys. Res. Lett. 39, DOI: 10.1029/2012gl053055.

Bowman, D., Boggs, G.S. and Prior, L.D., 2008. Fire maintains an *Acacia aneura* shrubland—*Triodia* grassland mosaic in central Australia. J. Arid. Environ. 72: 34–47, DOI: 10.1016/j.jaridenv.2007.04.001.

Bowman, D., Boggs, G.S., Prior, L.D. and Krull, E.S., 2007. Dynamics of *Acacia aneura-Triodia* boundaries using carbon (^{14}C and $\delta^{13}C$) and nitrogen ($\delta^{15}N$) signatures in soil organic matter in central Australia. Holocene. 17: 311–318, DOI: 10.1177/0959683607076442.

Bowman, D., Brown, G.K., Braby, M.F., Brown, J.R., Cook, L.G., Crisp, M.D., Ford, F., Haberle, S., Hughes, J., Isagi, Y., Joseph, L., McBride, J., Nelson, G. and Ladiges, P.Y., 2010. Biogeography of the Australian monsoon tropics. J. Biogeogr. 37: 201–216, DOI: 10.1111/j.1365-2699.2009.02210.x.

Breshears, D.D., Myers, O.B. and Barnes, F.J., 2009. Horizontal heterogeneity in the frequency of plant-available water with woodland intercanopy-canopy vegetation patch type rivals that occuring vertically by soil depth. Ecohydrology. 2: 503–519.

602   Calf, G.E., McDonald, P.S. and Jacobson, G., 1991. Recharge mechanism and
603   groundwater age in the Ti-Tree basin, Northern Territory. Aust. J. Earth Sci. 38: 299–306,
604   DOI: 10.1080/08120099108727974.

605   Campbell Scientific Inc., 2004. Open path eddy covariance system operator's
606   manual, Logan, UT, USA, pp. 60.

607   Chen, C., Eamus, D., Cleverly, J., Boulain, N., Cook, P., Zhang, L., Cheng, L. and
608   Yu, Q., 2014. Modelling vegetation water-use and groundwater recharge as affected by
609   climate variability in an arid-zone *Acacia* savanna woodland. J. Hydrol. 519: 1084–1096,
610   DOI: 10.1016/j.jhydrol.2014.08.032.

611   Cleverly, J., 2011. Alice Springs Mulga OzFlux site. OzFlux: Australian and New
612   Zealand Flux Research and Monitoring Network, hdl: 102.100.100/8697.

613   Cleverly, J., 2013. Ti Tree East OzFlux Site. OzFlux: Australian and New Zealand
614   Flux Research and Monitoring Network, hdl: 102.100.100/11135.

615   Cleverly, J., Boulain, N., Villalobos-Vega, R., Grant, N., Faux, R., Wood, C.,
616   Cook, P.G., Yu, Q., Leigh, A. and Eamus, D., 2013a. Dynamics of component carbon
617   fluxes in a semi-arid *Acacia* woodland, central Australia. J. Geophys. Res.-Biogeosci.
618   118: 1168–1185, DOI: 10.1002/jgrg.20101.

619   Cleverly, J., Chen, C., Boulain, N., Villalobos-Vega, R., Faux, R., Grant, N., Yu,
620   Q. and Eamus, D., 2013b. Aerodynamic resistance and Penman-Monteith
621   evapotranspiration over a seasonally two-layered canopy in semiarid central Australia. J.
622   Hydrometeor. 14: 1562–1570, DOI: 10.1175/jhm-d-13-080.1.

623   Cleverly, J. and Isaac, P., 2015. OzFluxQC Simulator version 2.8.6. GitHub
624   respository, github.com/james-cleverly/OzFluxQC_Simulator, DOI:
625   10.5281/zenodo.13730.

626   Cook, P.G. and O'Grady, A.P., 2006. Determining soil and ground water use of
627   vegetation from heat pulse, water potential and stable isotope data. Oecologia. 148: 97–
628   107, DOI: 10.1007/s00442-005-0353-4.

629   Cox, P.M., Pearson, D., Booth, B.B., Friedlingstein, P., Huntingford, C., Jones,
630   C.D. and Luke, C.M., 2013. Sensitivity of tropical carbon to climate change constrained
631   by carbon dioxide variability. Nature. 494: 341–344, DOI: 10.1038/nature11882.

632   Donohue, R.J., Hume, I.H., Roderick, M.L., McVicar, T.R., Beringer, J., Hutley,
633   L.B., Gallant, J.C., Austin, J.M., van Gorsel, E., Cleverly, J.R., Meyer, W.S. and Arndt,
634   S.K., 2014. Evaluation of the remote-sensing-based DIFFUSE model for estimating
635   photosynthesis of vegetation. Remote Sens. Environ. 155: 349–365, DOI:
636   10.1016/j.rse.2014.09.007.

637   Dunn, A.L., Barford, C.C., Wofsy, S.C., Goulden, M.L. and Daube, B.C., 2007. A
638   long-term record of carbon exchange in a boreal black spruce forest: means, responses to
639   interannual variability, and decadal trends. Glob. Change Biol. 13: 577–590, DOI:
640   10.1111/j.1365-2486.2006.01221.x.

641   Eamus, D., Cleverly, J., Boulain, N., Grant, N., Faux, R. and Villalobos-Vega, R.,
642 2013. Carbon and water fluxes in an arid-zone *Acacia* savanna woodland: An analyses of
643 seasonal patterns and responses to rainfall events. Agric. For. Meteor. 182–183: 225–238,
644 DOI: 10.1016/j.agrformet.2013.04.020.

645   Eamus, D., Hatton, T., Cook, P. and Colvin, C., 2006. Ecohydrology. Vegetation
646 function, water and resource management. CSIRO Publishing, Collingwood, VIC, 348 pp.

647   Fasullo, J.T., Boening, C., Landerer, F.W. and Nerem, R.S., 2013. Australia's
648 unique influence on global sea level in 2010-2011. Geophys. Res. Lett. 40: 4368-4373,
649 DOI: 10.1002/grl.50834.

650   Flanagan, L.B. and Adkinson, A.C., 2011. Interacting controls on productivity in a
651 northern Great Plains grassland and implications for response to ENSO events. Glob.
652 Change Biol. 17: 3293–3311, DOI: 10.1111/j.1365-2486.2011.02461.x.

653   Harrington, G.A., Cook, P.G. and Herczeg, A.L., 2002. Spatial and temporal
654 variability of ground water recharge in central Australia: A tracer approach. Ground
655 Water. 40: 518–527, DOI: 10.1111/j.1745-6584.2002.tb02536.x.

656   Hastings, S.J., Oechel, W.C. and Muhlia-Melo, A., 2005. Diurnal, seasonal and
657 annual variation in the net ecosystem CO_2 exchange of a desert shrub community
658 (Sarcocaulescent) in Baja California, Mexico. Glob. Change Biol. 11: 927–939, DOI:
659 10.1111/j.1365-2486.2005.00951.x.

660   Hsu, K.-l., Gupta, H.V., Gao, X., Sorooshian, S. and Imam, B., 2002. Self-
661 organizing linear output map (SOLO): An artificial neural network suitable for hydrologic
662 modeling and analysis. Water Resour. Res. 38: 1302, DOI: 10.1029/2001wr000795.

663   Huete, A., Didan, K., Miura, T., Rodriguez, E.P., Gao, X. and Ferreira, L.G., 2002.
664 Overview of the radiometric and biophysical performance of the MODIS vegetation
665 indices. Remote Sens. Environ. 83: 195–213, DOI: 10.1016/s0034-4257(02)00096-2.

666   Huxman, T.E., Snyder, K.A., Tissue, D., Leffler, A.J., Ogle, K., Pockman, W.T.,
667 Sandquist, D.R., Potts, D.L. and Schwinning, S., 2004. Precipitation pulses and carbon
668 fluxes in semiarid and arid ecosystems. Oecologia. 141: 254–268, DOI: 10.1007/s00442-
669 004-1682-4.

670   Kanniah, K.D., Beringer, J. and Hutley, L.B., 2010. The comparative role of key
671 environmental factors in determining savanna productivity and carbon fluxes: A review,
672 with special reference to Northern Australia. Progress in Physical Geography. 34: 459–
673 490.

674   Keenan, T.F., Gray, J., Friedl, M.A., Toomey, M., Bohrer, G., Hollinger, D.Y.,
675 Munger, J.W., O'Keefe, J., Schmid, H.P., Wing, I.S., Yang, B. and Richardson, A.D.,
676 2014. Net carbon uptake has increased through warming-induced changes in temperate
677 forest phenology. Nature Clim. Change. 4: 598–604, DOI: 10.1038/nclimate2253.

678   King, K.J., Cary, G.J., Bradstock, R.A. and Marsden-Smedley, J.B., 2013.
679 Contrasting fire responses to climate and management: insights from two Australian
680 ecosystems. Glob. Change Biol. 19: 1223–1235, DOI: 10.1111/gcb.12115.

681   Kljun, N., Calanca, P., Rotach, M.W. and Schmid, H.P., 2004. A simple
682   parameterisation for flux footprint predictions. Bound.-Lay. Meteor. 112: 503-523, DOI:
683   10.1023/b:boun.0000030653.71031.96.

684   Le Quéré, C., Peters, G.P., Andres, R.J., Andrew, R.M., Boden, T.A., Ciais, P.,
685   Friedlingstein, P., Houghton, R.A., Marland, G., Moriarty, R., Sitch, S., Tans, P., Arneth,
686   A., Arvanitis, A., Bakker, D.C.E., Bopp, L., Canadell, J.G., Chini, L.P., Doney, S.C.,
687   Harper, A., Harris, I., House, J.I., Jain, A.K., Jones, S.D., Kato, E., Keeling, R.F., Klein
688   Goldewijk, K., Körtzinger, A., Koven, C., Lefèvre, N., Maignan, F., Omar, A., Ono, T.,
689   Park, G.H., Pfeil, B., Poulter, B., Raupach, M.R., Regnier, P., Rödenbeck, C., Saito, S.,
690   Schwinger, J., Segschneider, J., Stocker, B.D., Takahashi, T., Tilbrook, B., van Heuven,
691   S., Viovy, N., Wanninkhof, R., Wiltshire, A. and Zaehle, S., 2014. Global carbon budget
692   2013. Earth Syst. Sci. Data. 6: 235–263, DOI: 10.5194/essd-6-235-2014.

693   Leffler, A.J. and Evans, A.S., 1999. Variation in carbon isotope composition
694   among years in the riparian tree *Populus fremontii*. Oecologia. 119: 311–319.

695   Loik, M.E., Breshears, D.D., Lauenroth, W.K. and Belnap, J., 2004. A multi-scale
696   perspective of water pulses in dryland ecosystems: climatology and ecohydrology of the
697   western USA. Oecologia. 141: 269–281.

698   Ludwig, J.A., Wilcox, B.P., Breshears, D.D., Tongway, D.J. and Imeson, A.C.,
699   2005. Vegetation patches and runoff-erosion as interacting ecohydrological processes in
700   semiarid landscapes. Ecology. 86: 288–297.

701   Luyssaert, S., Inglima, I., Jung, M., Richardson, A.D., Reichstein, M., Papale, D.,
702   Piao, S.L., Schulzes, E.D., Wingate, L., Matteucci, G., Aragao, L., Aubinet, M., Beers, C.,
703   Bernhofer, C., Black, K.G., Bonal, D., Bonnefond, J.M., Chambers, J., Ciais, P., Cook, B.,
704   Davis, K.J., Dolman, A.J., Gielen, B., Goulden, M., Grace, J., Granier, A., Grelle, A.,
705   Griffis, T., Grunwald, T., Guidolotti, G., Hanson, P.J., Harding, R., Hollinger, D.Y.,
706   Hutyra, L.R., Kolar, P., Kruijt, B., Kutsch, W., Lagergren, F., Laurila, T., Law, B.E., Le
707   Maire, G., Lindroth, A., Loustau, D., Malhi, Y., Mateus, J., Migliavacca, M., Misson, L.,
708   Montagnani, L., Moncrieff, J., Moors, E., Munger, J.W., Nikinmaa, E., Ollinger, S.V.,
709   Pita, G., Rebmann, C., Roupsard, O., Saigusa, N., Sanz, M.J., Seufert, G., Sierra, C.,
710   Smith, M.L., Tang, J., Valentini, R., Vesala, T. and Janssens, I.A., 2007. CO_2 balance of
711   boreal, temperate, and tropical forests derived from a global database. Glob. Change Biol.
712   13: 2509–2537, DOI: 10.1111/j.1365-2486.2007.01439.x.

713   Ma, J., Zheng, X.J. and Li, Y., 2012. The response of CO_2 flux to rain pulses at a
714   saline desert. Hydrol. Process. 26: 4029–4037, DOI: 10.1002/hyp.9204.

715   Ma, X., Huete, A., Yu, Q., Coupe, N.R., Davies, K., Broich, M., Ratana, P.,
716   Beringer, J., Hutley, L.B., Cleverly, J., Boulain, N. and Eamus, D., 2013. Spatial patterns
717   and temporal dynamics in savanna vegetation phenology across the North Australian
718   Tropical Transect. Remote Sens. Environ. 139: 97–115, DOI: 10.1016/j.rse.2013.07.030.

719   Ma, X., Huete, A., Yu, Q., Restrepo-Coupe, N., Beringer, J., Hutley, L.B.,
720   Kanniah, K.D., Cleverly, J. and Eamus, D., 2014. Parameterization of an ecosystem light-
721   use-efficiency model for predicting savanna GPP using MODIS EVI. Remote Sens.
722   Environ. 154: 253–271, DOI: 10.1016/j.rse.2014.08.025.

723   Maslin, B.R. and Reid, J.E., 2012. A taxonomic revision of Mulga (*Acacia aneura*
724 and its close relatives: Fabaceae) in Western Australia. Nuytsia. 22: 129–167.

725   Massman, W. and Clement, R., 2004. Uncertainty in eddy covariance flux
726 estimates resulting from spectral attenuation. In: X. Lee, W. Massman and B. Law
727 (Editors), Handbook of Micrometeorology: A guide for Surface Flux Measurement and
728 Analysis. Atmospheres and Oceanographic Sciences Library. Kluwer Academic
729 Publishers, Dordrecht/Boston/London, pp. 67–100.

730   Nano, C.E.M. and Clarke, P.J., 2010. Woody-grass ratios in a grassy arid system
731 are limited by multi-causal interactions of abiotic constraint, competition and fire.
732 Oecologia. 162: 719–732, DOI: 10.1007/s00442-009-1477-8.

733   Nemani, R.R., Keeling, C.D., Hashimoto, H., Jolly, W.M., Piper, S.C., Tucker,
734 C.J., Myneni, R.B. and Running, S.W., 2003. Climate-driven increases in global terrestrial
735 net primary production from 1982 to 1999. Science. 300: 1560–1563, DOI:
736 10.1126/science.1082750.

737   Nix, H.A. and Austin, M.P., 1973. Mulga: a bioclimatic analysis. Tropical
738 Grasslands. 7: 9–20.

739   O'Grady, A.P., Cook, P.G., Eamus, D., Duguid, A., Wischusen, J.D.H., Fass, T.
740 and Worldege, D., 2009. Convergence of tree water use within an arid-zone woodland.
741 Oecologia. 160: 643–655, DOI: 10.1007/s00442-009-1332-y.

742   O'Grady, A.P., Cook, P.G., Howe, P. and Werren, G., 2006a. Groundwater use by
743 dominant tree species in tropical remnant vegetation communities. Aust. J. Bot. 54: 155–
744 171, DOI: 10.1071/bt04179.

745   O'Grady, A.P., Eamus, D., Cook, P.G. and Lamontagne, S., 2006b. Comparative
746 water use by the riparian trees *Melaleuca argentea* and *Corymbia bella* in the wet-dry
747 tropics of northern Australia. Tree Physiol. 26: 219–228.

748   Peñuelas, J., Terradas, J. and Lloret, F., 2011. Solving the conundrum of plant
749 species coexistence: water in space and time matters most. New Phytol. 189: 5-8, DOI:
750 10.1111/j.1469-8137.2010.03570.x.

751   Ponce Campos, G.E., Moran, M.S., Huete, A., Zhang, Y., Bresloff, C., Huxman,
752 T.E., Eamus, D., Bosch, D.D., Buda, A.R., Gunter, S.A., Scalley, T.H., Kitchen, S.G.,
753 McClaran, M.P., McNab, W.H., Montoya, D.S., Morgan, J.A., Peters, D.P.C., Sadler, E.J.,
754 Seyfried, M.S. and Starks, P.J., 2013. Ecosystem resilience despite large–scale altered
755 hydroclimate conditions. Nature. 494: 349–352, DOI: 10.1038/nature11836.

756   Poulter, B., Frank, D., Ciais, P., Myneni, R.B., Andela, N., Bi, J., Broquet, G.,
757 Canadell, J.G., Chevallier, F., Liu, Y.Y., Running, S.W., Sitch, S. and van der Werf, G.R.,
758 2014. Contribution of semi-arid ecosystems to interannual variability of the global carbon
759 cycle. Nature. 509: 600–603, DOI: 10.1038/nature13376.

760   Pressland, A.J., 1975. Productivity and management of Mulga in south-western
761 Queensland in relation to tree structure and density. Aust. J. Bot. 23: 965–976, DOI:
762 10.1071/bt9750965.

763   Reid, N., Hill, S.M. and Lewis, D.M., 2008. Spinifex biogeochemical expressions
764 of buried gold mineralisation: The great mineral exploration penetrator of transported
765 regolith. Appl. Geochem. 23: 76–84, DOI: 10.1016/j.apgeochem.2007.09.007.

766   Reynolds, J.F., Kemp, P.R., Ogle, K. and Fernandez, R.J., 2004. Modifying the
767 'pulse-reserve' paradigm for deserts of North America: precipitation pulses, soil water, and
768 plant responses. Oecologia. 141: 194–210.

769   Reynolds, J.F., Stafford Smith, D.M., Lambin, E.F., Turner, B.L., Mortimore, M.,
770 Batterbury, S.P.J., Downing, T.E., Dowlatabadi, H., Fernandez, R.J., Herrick, J.E., Huber-
771 Sannwald, E., Jiang, H., Leemans, R., Lynam, T., Maestre, F.T., Ayarza, M. and Walker,
772 B., 2007. Global desertification: Building a science for dryland development. Science.
773 316: 847–851, DOI: 10.1126/science.1131634.

774   Rutledge, S., Campbell, D.I., Baldocchi, D. and Schipper, L.A., 2010.
775 Photodegradation leads to increased carbon dioxide losses from terrestrial organic matter.
776 Glob. Change Biol. 16: 3065–3074, DOI: 10.1111/j.1365-2486.2009.02149.x.

777   Scanlon, B.R., Keese, K.E., Flint, A.L., Flint, L.E., Gaye, C.B., Edmunds, W.M.
778 and Simmers, I., 2006. Global synthesis of groundwater recharge in semiarid and arid
779 regions. Hydrol. Process. 20: 3335–3370, DOI: 10.1002/hyp.6335.

780   Schlesinger, C., White, S. and Muldoon, S., 2013. Spatial pattern and severity of
781 fire in areas with and without buffel grass (*Cenchrus ciliaris*) and effects on native
782 vegetation in central Australia. Austral Ecol. 38: 831–840, DOI: 10.1111/aec.12039.

783   Schotanus, P., Nieuwstadt, F.T.M. and Debruin, H.A.R., 1983. Temperature-
784 measurement with a sonic anemometer and its application to heat and moisture fluxes.
785 Bound.-Lay. Meteor. 26: 81–93.

786   Taylor, D. and Eamus, D., 2008. Coordinating leaf functional traits with branch
787 hydraulic conductivity: resource substitution and implications for carbon gain. Tree
788 Physiol. 28: 1169–1177.

789   Thiry, M., Milnes, A.R., Rayot, V. and Simon-Coincon, R., 2006. Interpretation of
790 palaeoweathering features and successive silicifications in the Tertiary regolith of inland
791 Australia. J. Geol. Soc. 163: 723–736, DOI: 10.1144/0014-764905-020.

792   Tongway, D.J. and Ludwig, J.A., 1990. Vegetation and soil patterning in semiarid
793 mulga lands of Eastern Australia. Aust. J. Ecol. 15: 23–34, DOI: 10.1111/j.1442-
794 9993.1990.tb01017.x.

795   van Dijk, A., Dolman, A.J. and Schulze, E.D., 2005. Radiation, temperature, and
796 leaf area explain ecosystem carbon fluxes in boreal and temperate European forests. Glob.
797 Biogeochem. Cycle. 19: GB2029, DOI: 10.1029/2004gb002417.

798   Vanderbilt, K.L., White, C.S., Hopkins, O. and Craig, J.A., 2008. Aboveground
799 decomposition in arid environments: Results of a long-term study in central New Mexico.
800 J. Arid. Environ. 72: 696–709.

801   Warner, T.T., 2004. Desert Meteorology. Cambridge University Press, Cambridge
802 UK, 595 pp.

803   Webb, E., Pearman, G. and Leuning, R., 1980. Correction of flux measurements
804 for density effects due to heat and water-vapor transfer. Q. J. Roy. Meteor. Soc. 106: 85–
805 100.

806   Wesely, M.L., 1970. Eddy correlation measurements in the atmospheric surface
807 layer over agricultural crops. Ph.D. Dissertation Thesis, University of Wisconsin,
808 Madison, 102 pp.

809   Whitley, R.J., Macinnis-Ng, C.M.O., Hutley, L.B., Beringer, J., Zeppel, M.,
810 Williams, M., Taylor, D. and Eamus, D., 2011. Is productivity of mesic savannas light
811 limited or water limited? Results of a simulation study. Glob. Change Biol. 17: 3130–
812 3149, DOI: 10.1111/j.1365-2486.2011.02425.x.

813   Winkworth, R.E., 1973. Eco-physiology of Mulga (*Acacia aneura*). Tropical
814 Grasslands. 7: 43–48.

815   Wright, I.J., Falster, D.S., Pickup, M. and Westoby, M., 2006. Cross-species
816 patterns in the coordination between leaf and stem traits, and their implications for plant
817 hydraulics. Physiologia Plantarum. 127: 445–456, DOI: 10.1111/j.1399-
818 3054.2006.00699.x.

819   Zha, T.S., Li, C.Y., Kellomaki, S., Peltola, H., Wang, K.Y. and Zhang, Y.Q., 2013.
820 Controls of evapotranspiration and CO_2 fluxes from Scots pine by surface conductance
821 and abiotic factors. PLoS ONE. 8: e69027, DOI: 10.1371/journal.pone.0069027.

822   Zhang, Y.J., Meinzer, F.C., Hao, G.Y., Scholz, F.G., Bucci, S.J., Takahashi,
823 F.S.C., Villalobos-Vega, R., Giraldo, J.P., Cao, K.F., Hoffmann, W.A. and Goldstein, G.,
824 2009. Size-dependent mortality in a Neotropical savanna tree: the role of height-related
825 adjustments in hydraulic architecture and carbon allocation. Plant Cell Environ. 32: 1456–
826 1466, DOI: 10.1111/j.1365-3040.2009.02012.x.

827   Zhao, M.S. and Running, S.W., 2010. Drought-induced reduction in global
828 terrestrial net primary production from 2000 through 2009. Science. 329: 940–943, DOI:
829 10.1126/science.1192666.

830   Zolfaghar, S., Villalobos-Vega, R., Cleverly, J., Zeppel, M., Rumman, R. and
831 Eamus, D., 2014. The influence of depth-to-groundwater on structure and productivity of
832 *Eucalyptus* woodlands. Aust. J. Bot. 62: 428-437, DOI: 10.1071/BT14139.

833

834

835

836

8. Legends

Table 1. Summary of rainfall and net ecosystem productivity (NEP) for four years of study at the Mulga woodland. Data for 2010–2012 from Eamus *et al*. (2013) and Cleverly *et al*. (2013a).

Figure 1. Daily (a, b) and cumulative (c) precipitation in the Mulga woodland (a, solid line c) and the *Corymbia* savanna (b, broken line c).

Figure 2. Daily (a) and cumulative (b) evapotranspiration (ET) in the Mulga woodland (solid line) and the *Corymbia* savanna (broken line).

Figure 3. Daily (a) and cumulative (b) net ecosystem productivity (NEP) in the Mulga woodland (solid line) and the *Corymbia* savanna (broken line). Daily values are shown as the 3-day running average. Values of NEP that are larger than zero (dashed line) represent C uptake.

Figure 4. Daily cycle of NEP. Values represent hourly average ± standard error (s.e.) during January 2013.

Figure 5. Daily ecosystem water use efficiency (eWUE). Values were determined as NEP/ET and shown for days when $ET > 0.2$ mm d^{-1}. Values above zero (dashed line) represent photosynthetic eWUE, while increasingly negative values of eWUE represent increasing values of respiratory eWUE.

Figure 6. MODIS enhanced vegetation index (EVI) as a four-month running average.

Figure 7. Carbon stable isotope ratio ($\delta^{13}C$) of *Acacia* (squares) and *C. opaca* (circles) leaves in the Mulga woodland and across three habitats (Mulga patch, open savanna, transition) within the *Corymbia* savanna. Symbols show mean ± s.e.
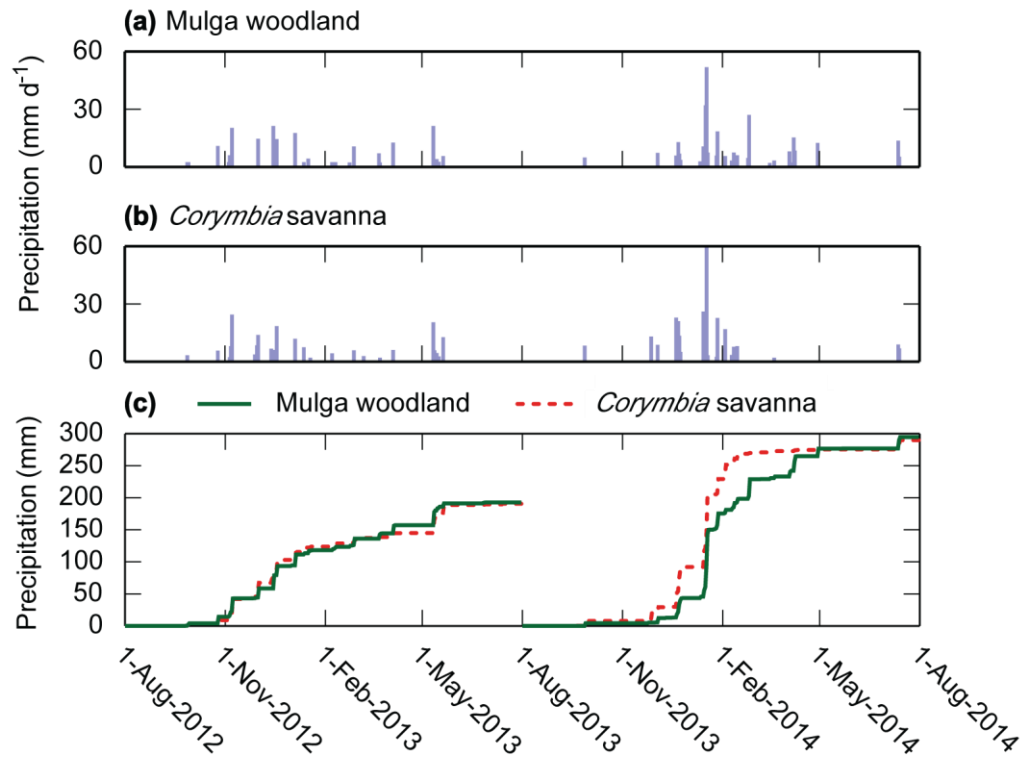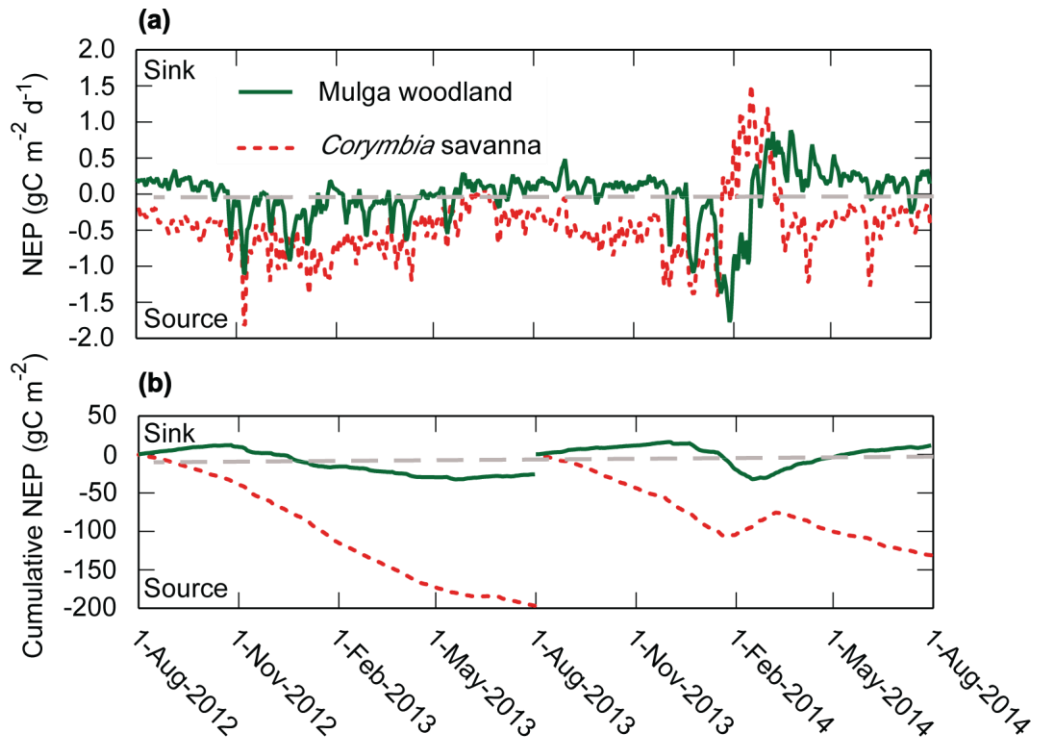
862   Table 1. Summary of rainfall and net ecosystem productivity (NEP) for four years

863   of study at the Mulga woodland. Data for 2010–2012 are from Eamus et al. (2013) and

864   Cleverly et al. (2013a). Data for 2012–2014 are from this study.

865

Year	Rainfall (mm y^{-1})	NEP (g C m^{-2} y^{-1})
2010–2011	565	259
2011–2012	184	−4
2012–2013	193	−25
2013–2014	295	12

866

867

Figure 1. Daily (a, b) and cumulative (c) precipitation in the Mulga woodland (a, solid line c) and the *Corymbia* savanna (b, broken line c).
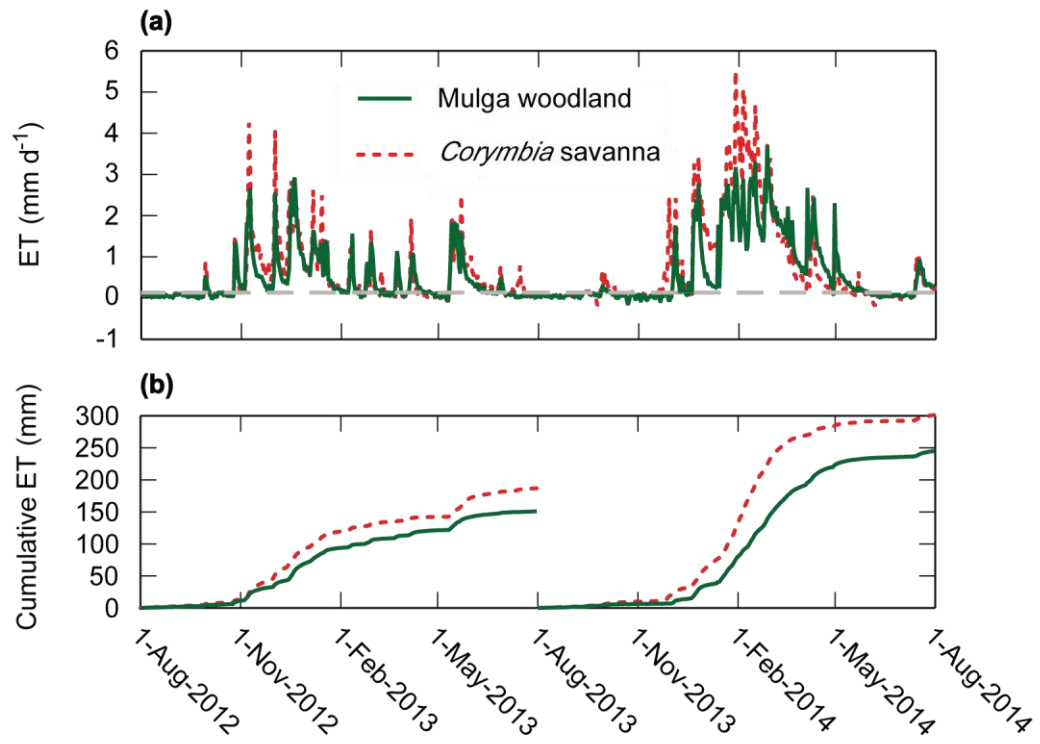
872

873   Figure 2. Daily (a) and cumulative (b) evapotranspiration (ET) in the Mulga

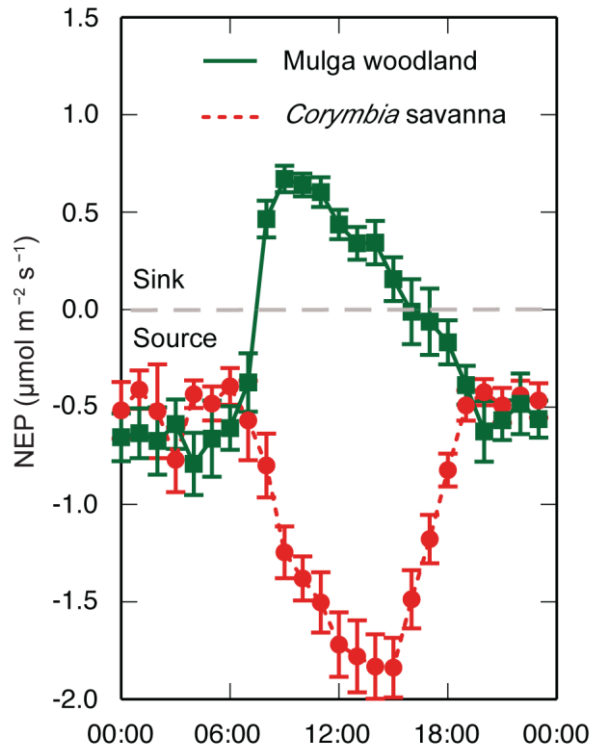874   woodland (solid line) and the *Corymbia* savanna (broken line).

875

876

877   Figure 3. Daily (a) and cumulative (b) net ecosystem productivity (NEP) in the

878   Mulga woodland (solid line) and the *Corymbia* savanna (broken line). Daily values are

879   shown as the 3-day running average. Values of NEP that are larger than zero (dashed line)
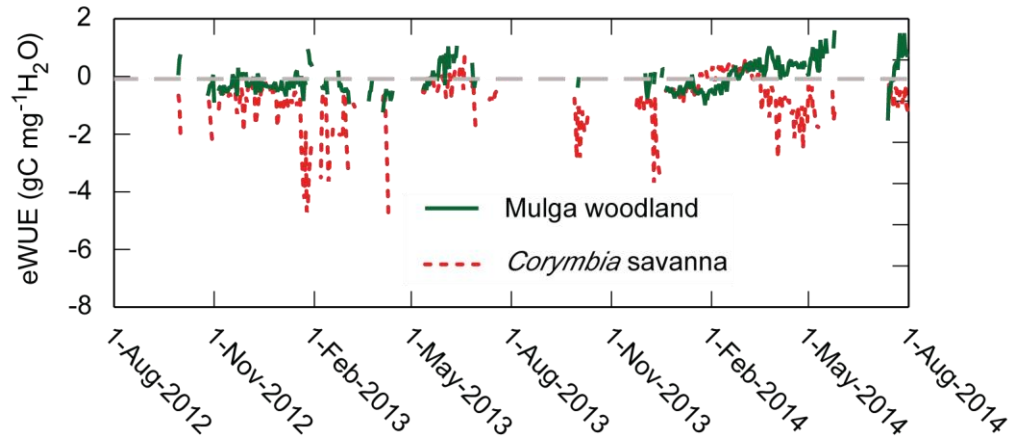
880   represent C uptake.

881

882

883   Figure 4. Daily cycle of NEP. Values represent hourly average ± standard error
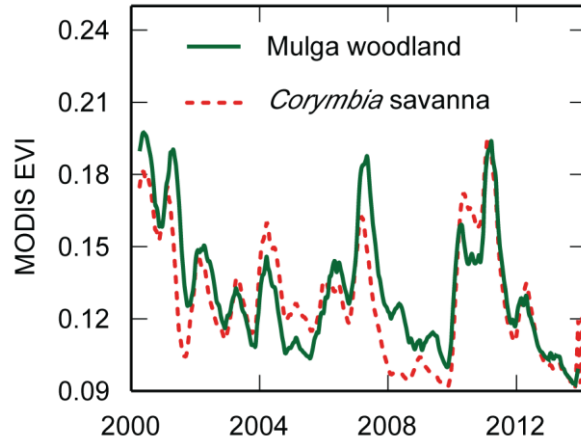
884   (s.e.) during January 2013.

885

886

887   Figure 5. Daily ecosystem water use efficiency (eWUE). Values were determined

888   as NEP/ET and shown for days when $ET > 0.2$ mm d^{-1}. Values above zero (dashed line)

889   represent photosynthetic eWUE, while increasingly negative values of eWUE represent

890   increasing values of respiratory eWUE.
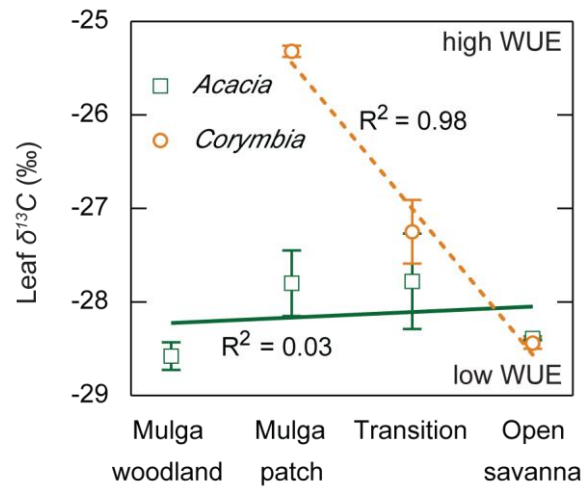
891

892

893   Figure 6. MODIS enhanced vegetation index (EVI) as a four-month running

894   average.

895

896

897   Figure 7. Carbon stable isotope ratio ($\delta^{13}C$) of *Acacia* (squares) and *C. opaca*

898   (circles) leaves in the Mulga woodland and across three habitats (Mulga patch, open

899   savanna, transition) within the *Corymbia* savanna. Symbols show mean ± s.e.

900

901